

FRET-Based Mito-Specific Fluorescent Probe for Ratiometric Detection and Imaging of Endogenous Peroxynitrite: Dyad of Cy3 and Cy5

Xiaotong Jia,[†] Qiangqiang Chen,[‡] Yingfang Yang,[‡] Yao Tang,[†] Rui Wang,[‡] Yufang Xu,[†] Weiping Zhu,[†] and Xuhong Qian^{*,†}

[†]State Key Laboratory of Bioreactor Engineering, Shanghai Key Laboratory of Chemical Biology, and [‡]Shanghai Key Laboratory of New Drug Design, School of Pharmacy, East China University of Science and Technology, Meilong Road 130, Shanghai 200237, China

S Supporting Information

ABSTRACT: Peroxynitrite (OONO⁻) is profoundly implicated in health and disease. The physiological and pathological outcome of OONO⁻ is related to its local concentration, and hence, a reliable OONO⁻ assay is highly desired. We have developed a FRET-based small-molecule fluorescent probe (PNCy3Cy5), harnessing the differential reactivity of Cy3 and Cy5 toward OONO⁻ by fine-tuning. It exhibits high detection sensitivity and yields a ratiometric fluorescent signal. We have exemplified that it can be applied in semiquantitative determination of OONO⁻ in living cells. Notably, it specifically localizes in mitochondria, where endogenous OONO⁻ is predominantly generated. Thus, PNCy3Cy5 is a promising molecular tool for peroxynitrite biology.

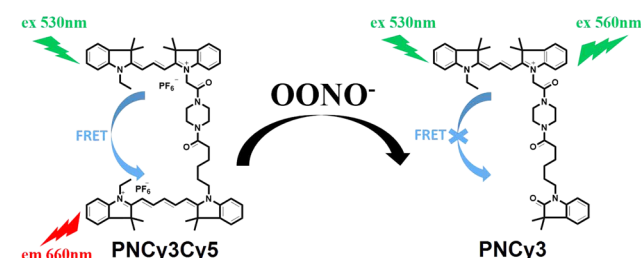
Peroxynitrite (OONO⁻) is endogenously produced in living systems by the diffusion-controlled coupling of nitric oxide (*NO) and superoxide radical anion (O₂^{-•}).¹ Though the cytotoxicity of OONO⁻ plays a key role in signal transduction and antimicrobial activities,² excessive OONO⁻ can damage critical cell components, including proteins, DNA, lipids, iron–sulfur clusters, and thiols. The accumulation of cell injuries eventually leads to apoptosis and necrosis.³ Mounting evidence have established a firm correlation between OONO⁻ and a number of pathological conditions, such as cardiovascular diseases, neurodegenerative diseases, chronic inflammation, ischemia reperfusion injury, and diabetes.⁴ Therefore, assays for OONO⁻ detection are important for elucidating pathophysiology of OONO⁻ and may be used for peroxynitrite-related disease diagnosis.

Recently, there have emerged a number of fluorescent probes for OONO⁻,⁵ and some of them have been used for biomedical studies.⁶ Most of these probes exhibit a turn-on fluorescence signal at a single channel. The scope of such probes in quantitative *in vitro* studies is limited due to complications by photobleaching, uneven loading, or fluctuation in excitation intensity.⁷ In comparison, probes based on two-channel ratiometric signal address these complications by allowing self-calibration. Recently, we and other groups have reported a few reaction-based⁸ small-molecule and semiconducting polymer probes for ratiometric detecting OONO⁻.^{9–11} Nevertheless, it

remains challenging to design robust assays for determining OONO⁻ levels in living cells.

We present herein the first FRET-based small-molecule ratiometric fluorescent probe (PNCy3Cy5) for detection of OONO⁻ (Scheme 1). It specifically localizes at mitochondria,

Scheme 1. Structure of PNCy3Cy5 and Its Detection Mechanism



the major sources of endogenous OONO⁻. It also exhibits high detection sensitivity and applications for semiquantitative detection of OONO⁻ in living cells.

The ratiometric detection mechanism of PNCy3Cy5 is based on modulating FRET between Cy3 and Cy5. The photofading and photoswitching of cyanine dyes are caused mainly by oxidants and nucleophiles, through cleaving or forming adducts of polymethine bridge.¹² The chemostability of a polymethine cyanine dye toward oxidants deteriorates as its conjugative backbone elongates.¹² Nagano et al. reported that Cy5 and Cy7 are both readily oxidized by OONO⁻ and that Cy7 is more susceptible than Cy5.^{5a} We envisioned that Cy3, which has shorter polymethine chain, may show better stability to OONO⁻. The reactivity of Cy3 and Cy5 to OONO⁻ was tested in physiological pH. In contrast to Cy5, the UV–vis absorption of Cy3 remained unchanged even with addition of 50 equiv of OONO⁻, which is consistent with our hypothesis (Figure S2). This result suggests the possibility to create a OONO⁻ probe by fine-tuning reactivity of Cy3 and Cy5. Also, Cy3 and Cy5 are a popular pair of FRET fluorophores. Therefore, it is possible to design covalent Cy3–Cy5 to achieve a FRET-based ratiometric probe for OONO⁻. The judicious choice of linker between Cy3

Received: June 21, 2016

Published: August 12, 2016

and Cy5 is also a key factor determining the energy transfer efficiency. Moerner et al. and Squier et al. have employed the hexanoyl-hydrazine/ethylenediamine-hexanoyl spacer to tether Cy3–Cy5.¹³ The latter linker is long at ca. 21 Å. We chose a shorter acetyl-piperazyl-hexanoyl linker of ca. 14 Å in hope for enhancing FRET efficiency, as which is inversely proportional to the sixth power of the distance between the FRET pair.¹⁴

The spectral properties of PNCy3Cy5 were first examined in 0.1 M phosphate buffer (pH = 7.4, 0.2% DMF, v/v). It exhibits two absorption maxima at 540 nm and at 640 nm, which respectively correspond to those of the Cy3 and Cy5 units in its scaffold. When PNCy3Cy5 was excited at 530 nm, which efficiently excites Cy3 but not Cy5, an intense fluorescence emission of Cy5 at 660 nm was observed, but not that of Cy3 at 560 nm. This indicates efficient energy transfer between Cy3 donor and Cy5 acceptor (Figure S8). Upon addition of OONO⁻ (0–5 equiv), the absorption intensity of PNCy3Cy5 at 640 nm decreased, while the absorption band at 540 nm remained unaffected (Figure 1a). Concomitantly, the color of the solution

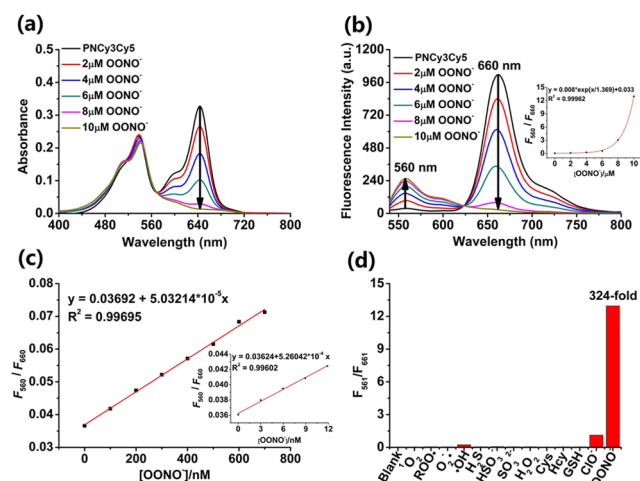


Figure 1. (a) UV–vis absorption spectra of PNCy3Cy5 (2 μM) to OONO⁻ (0–5 equiv). (b) Fluorescence spectra of PNCy3Cy5 (2 μM) to OONO⁻ (0–5 equiv); inset shows the plot of emission ratio (F_{560}/F_{660}) to OONO⁻ (0–10 μM), λ_{ex} = 530 nm. (c) Linear relationship of emission intensity ratio (F_{560}/F_{660}) to OONO⁻ (0–700 nM); inset shows the linear response to lower OONO⁻ (0–12 nM). (d) Emission intensity ratio (F_{560}/F_{660}) of PNCy3Cy5 (2 μM) in the presence of various ROS and some physiological nucleophiles (5 equiv for ClO⁻ and OONO⁻; 100 equiv for other species). Data were collected at 25 °C in 0.1 M phosphate buffer (pH = 7.4, 0.2% DMF, v/v) within 30 s.

changes from dark purple to pink. Fluorescence titration of a solution of PNCy3Cy5 with OONO⁻ demonstrated a decrease of the emission band at 660 nm and increase at 560 nm (Figure 1b). The fluorescence intensity ratio between 560 and 660 nm (F_{560}/F_{660}) exhibited a nearly 324-fold enhancement, from 0.04 in the absence of OONO⁻ to 12.96 upon addition of OONO⁻ (5 equiv) (Figure 1d). The emission intensity ratio has an excellent linear relationship with OONO⁻ in 0–700 nM (Figure 1c). The detection limit of PNCy3Cy5 for OONO⁻ was tested to be as low as 0.65 nM (Figure 1c, inset). The detection mechanism of PNCy3Cy5 toward OONO⁻ was in agreement with literature precedents.^{12c} The structure of the detection product (PNCy3) was further unambiguously confirmed by MALDI-TOF ($[M]^+ = m/z$ 740.4025).

Reactivity of PNCy3Cy5 toward various potentially interfering species, including ROSs and physiological nucleophiles, were

tested (Figure 1d, Figure S11). ClO⁻ up to 5 equiv induced a minor signal enhancement of 28-fold, while OONO⁻ triggered a remarkable enhancement of emission ratio F_{560}/F_{660} of over 300-fold as we have noted. Spectral changes induced by addition of other various ROSs up to 100 equiv, including H₂O₂, O₂^{-•}, •OH, ¹O₂, and ROO[•], are not discernible. Other physiological nucleophiles, such as HSO₃⁻, SO₃²⁻, H₂S, Cys, Hcy, and GSH also induced no obvious changes.

The colocalization experiments of PNCy3Cy5 were performed in RAW264.7 by costaining with commercially available Mito-Tracker Green, Lyso-Tracker Green, and Hoechst 33342 (a nucleus-specific dye) (Figure 2). The red-channel fluores-

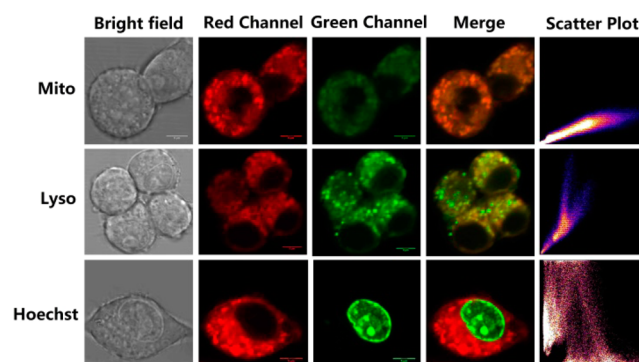


Figure 2. Confocal fluorescence images for intracellular localization of PNCy3Cy5 in macrophages. Cells were treated with 10 μM PNCy3Cy5 for 0.5 h and stained (0.5 h) with 200 nM Mito-Tracker Green, 200 nM Lyso-Tracker DND-26, or 5 $\mu\text{g}/\text{mL}$ Hoechst 33342. Red channel at 640–680 nm. Green channel at 500–540 nm for Mito-Tracker Green and Lyso-Tracker Green, 440–480 nm for Hoechst 33342.

cence of PNCy3Cy5 showed excellent overlay with green-channel fluorescence of Mito-Tracker Green, with Pearson's correlation coefficient at 0.94 ± 0.04 (evaluated by ImageJ software), probably due to the ammonium cation of cyanine fluorophore.^{5d,15} Comparatively, no good overlap was observed between PNCy3Cy5 and Lyso-Tracker Green or Hoechst 33342. In addition, the low cytotoxicity of PNCy3Cy5 was also demonstrated by MTT assay (Figure S1).

The ability of PNCy3Cy5 for ratiometric fluorescence detection of exogenous OONO⁻ in living cells was examined. RAW264.7 loaded with PNCy3Cy5 alone showed negligible fluorescence in green channel and strong fluorescence in red channel (Figure 3A,G). A dramatic drop of the red channel fluorescence and remarkable enhancement in the green channel fluorescence were observed in cells treated with SIN-1, a OONO⁻ donor (Figure 3B,C). The maximal production rate of OONO⁻ from SIN-1 was reported to be ca. 1.4% of initial SIN-1 concentration.¹⁶ However, cells treated with NOC-18 (diethylenetriamine), a NO[•] donor (Figure 3D,G) and MSB (menadione sodium bisulfite), a O₂^{-•} donor (Figure 3E,G) were almost unaffected. In SIN-1 treated cells, a 4.8-fold and a 29-fold and enhancement in the fluorescence ratio were observed (Figure 3G). We also found that the enhancement in the fluorescence ratio (green/red channel) shows a linear relationship with the dose of SIN-1, suggesting that PNCy3Cy5 is potentially suitable for semiquantitative studies (Figure 3H). Furthermore, the enhancement in emission ratio induced by SIN-1 was significantly abated by the presence of minocycline, a OONO⁻ scavenger (Figure 3F,G). These results suggest that

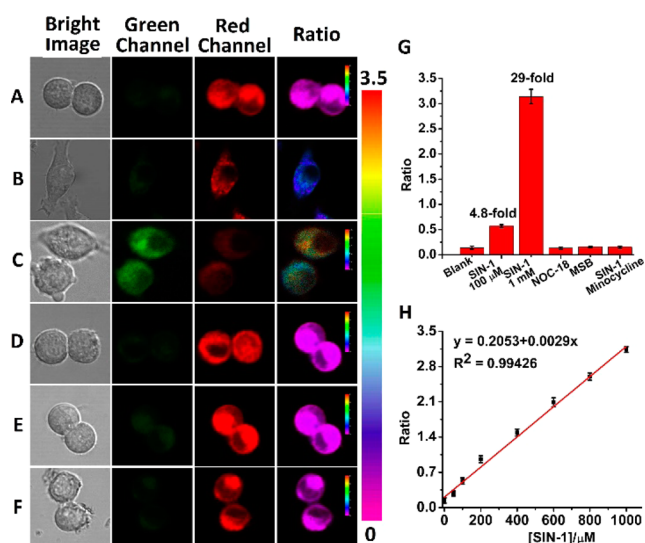


Figure 3. Confocal fluorescence imaging of PNCy3Cy5 selectivity with various exogenous ROS donors in RAW264.7 macrophages. Cells were treated with 10 μ M PNCy3Cy5 for 0.5 h and then corresponding stimulus for 2 h. (A) Control; (B) 100 μ M SIN-1; (C) 1 mM SIN-1; (D) 500 μ M NOC-18; (E) 100 μ M MSB; (F) 1 mM SIN-1 and 100 μ M minocycline. Green channel at 540–580 nm; red channel at 640–680 nm. Ratio images generated from green/red channel. (G) Average intensity ratios from ratio images of A–F. (H) Linear relationship of average intensity ratio with SIN-1 concentration. Error bars represent standard deviation.

PNCy3Cy5 can specifically and semiquantitatively detect and image exogenous OONO⁻ in living cells.

Next, the potentials of PNCy3Cy5 in detection of endogenously generated OONO⁻ was evaluated in RAW264.7 macrophages, which is known to release OONO⁻ upon stimulation of lipopolysaccharide (LPS)/interferon- γ (IFN- γ) and phorbol 12-myristate 13-acetate (PMA).¹⁷ It is assumed that the formation of OONO⁻ in stimulated macrophages can be regulated by nitric oxide synthase (iNOS) and NADPH oxidase (NOX).¹⁷ In RAW264.7 treated with only PNCy3Cy5, a slight green emission and strong red emission were observed (Figure 4A,E). Upon incubation with LPS/IFN- γ for 4 h and then PNCy3Cy5 and PMA, RAW264.7 showed a marked decrease in red channel and a dramatic increase in green channel, resulting in a 22-fold enhancement of emission ratio (Figure 4B,E). With the equation in Figure 3H, the level of endogenous OONO⁻ from stimulated cells was equivalent to that from ca. 760 μ M SIN-1 treated cells. As expected, cells pretreated with iNOS inhibitor (1400W) (Figure 4C,E) or NOX inhibitor (apocynin) (Figure 4D,E) accompanied by LPS/IFN- γ stimulation, and then PNCy3Cy5 and PMA, did not trigger the distinguishable increase of emission ratio. These results suggest that PNCy3Cy5 is a sensitive fluorescent probe capable of detecting the endogenous OONO⁻ in living systems.

It is known that mitochondria are the primary sources of peroxynitrite. OONO⁻ could induce mitochondria damages by oxidation, nitration and nitrosation of mitochondrial components.¹⁸ The performance of PNCy3Cy5 for endogenous OONO⁻ in mitochondria was established. RAW264.7 treated with free PNCy3Cy5 showed weak green fluorescence and intense red fluorescence (Figure 5A). In RAW264.7 stimulated with LPS/IFN- γ for 4 h and then PNCy3Cy5 and PMA, it was observed that red emission diminished and green emission increased significantly, along with outstanding overlay with blue

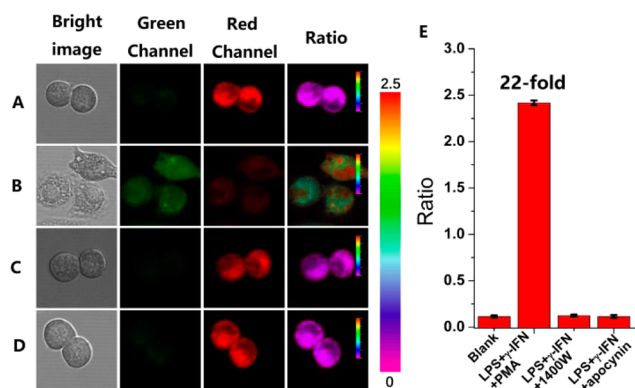


Figure 4. Confocal fluorescence imaging of endogenous OONO⁻ with PNCy3Cy5 in stimulated RAW264.7 macrophages. Normal cells (A) were treated with only 10 μ M PNCy3Cy5 for 0.5 h. Stimulated cells (B–D) were treated with 1 μ g/mL LPS, 50 ng/mL γ -IFN, and various inhibitors for 4 h, then 10 μ M PNCy3Cy5 for 0.5 h, following 20 nM PMA for 0.5 h. (A) Control; (B) LPS/ γ -IFN; (C) LPS/ γ -IFN and 100 nM 1400W; (D) LPS/ γ -IFN and 100 μ M apocynin. Green channel at 540–580 nm; red channel at 640–680 nm. Ratio images generated from green/red channel. (E) Average intensity ratios from ratio images of A–D. Error bars represent standard deviation.

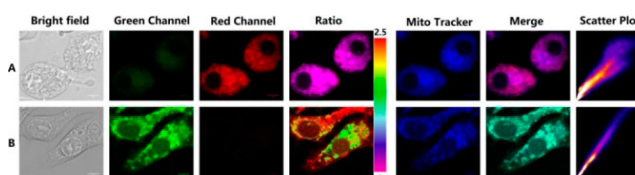


Figure 5. Confocal fluorescence imaging of endogenous OONO⁻ with PNCy3Cy5 at mitochondria in stimulated RAW264.7 macrophages. Cells were treated with 1 μ g/mL LPS, 50 ng/mL γ -IFN for 4 h, 10 μ M PNCy3Cy5 for 0.5 h, 20 nM PMA for 0.5 h, and then stained with 200 nM Mito-Tracker Green for 0.5 h. (A) Control; (B) LPS/ γ -IFN and PMA. Green Channel at 540–580 nm; red channel at 640–680 nm; ratio images generated from green/red channel.

fluorescence from Mito-Tracker Green. To the best of our knowledge, it has not been reported previously a small-molecule probe for ratiometric imaging of endogenous OONO⁻ in mitochondria.

In conclusion, we have developed a FRET-based fine-tuning reactivity probe (PNCy3Cy5) for ratiometric detection of peroxynitrite. In the presence of OONO⁻, a fluorescence intensity increase at 560 nm and a decrease at 660 nm were observed. The emission ratio (F_{560}/F_{660}) displays a large dynamic increase of up to 324-fold. An excellent detection limit of 0.65 nM was measured. PNCy3Cy5 is feasible for cellular imaging studies. It freely permeates cell membrane and specifically localizes in mitochondria, the major source of endogenous peroxynitrite. PNCy3Cy5 can be used in semiquantification of cellular OONO⁻ because the emission ratio of the green channel (540–580 nm) and red channel (640–680 nm) is linear to the concentration of added SIN-1. With PNCy3Cy5, the endogenous OONO⁻ generated in stimulated macrophage cells was successfully detected. These results make it a promising candidate for elucidating the involvement of OONO⁻ in various biological processes in living cells.

■ ASSOCIATED CONTENT

Supporting Information

The Supporting Information is available free of charge on the ACS Publications website at DOI: [10.1021/jacs.6b06398](https://doi.org/10.1021/jacs.6b06398).

Experimental details for chemical synthesis of all compounds, supplementary absorption and fluorescent characterization of probe and intermediates to ROSSs, and imaging methods and data (PDF)

■ AUTHOR INFORMATION

Corresponding Author

*xhqian@ecust.edu.cn

Notes

The authors declare no competing financial interest.

■ ACKNOWLEDGMENTS

This work was supported by the financial support from National Natural Science Foundation of China (21236002, 21476077, and 21302125), and the Fundamental Research Funds for the Central Universities. We thank Prof. Youjun Yang for insightful discussions and help with manuscript preparation.

■ REFERENCES

- (1) (a) Beckman, J. S.; Beckman, T. W.; Chen, J.; Marshall, P. A.; Freeman, B. A. *Proc. Natl. Acad. Sci. U. S. A.* **1990**, *87*, 1620. (b) Blough, N. V.; Zafiriou, O. C. *Inorg. Chem.* **1985**, *24*, 3502. (c) Huie, R. E.; Padmaja, S. *Free Radical Res. Commun.* **1993**, *18*, 195.
- (2) (a) Liaudet, L.; Vassalli, G.; Pacher, P. *Front. Biosci., Landmark Ed.* **2009**, *14*, 4809. (b) Radi, R. *J. Biol. Chem.* **2013**, *288*, 26464.
- (3) (a) Beckman, J. S. *Chem. Res. Toxicol.* **1996**, *9*, 836. (b) Radi, R. *Acc. Chem. Res.* **2013**, *46*, 550. (c) Wood, Z. A.; Schroder, E.; Robin Harris, J.; Poole, L. B. *Trends Biochem. Sci.* **2003**, *28*, 32. (d) Koppenol, W. H.; Moreno, J. J.; Pryor, W. A.; Ischiropoulos, H.; Beckman, J. S. *Chem. Res. Toxicol.* **1992**, *5*, 834.
- (4) (a) Pacher, P.; Beckman, J. S.; Liaudet, L. *Physiol. Rev.* **2007**, *87*, 315. (c) Szabó, C.; Ischiropoulos, H.; Radi, R. *Nat. Rev. Drug Discovery* **2007**, *6*, 662.
- (5) (a) Oushiki, D.; Kojima, H.; Terai, T.; Arita, M.; Hanaoka, K.; Urano, Y.; Nagano, T. *J. Am. Chem. Soc.* **2010**, *132*, 2795. (b) Xu, K.; Chen, H.; Tian, J.; Ding, B.; Xie, Y.; Qiang, M.; Tang, B. *Chem. Commun.* **2011**, *47*, 9468. (c) Chen, Z.-J.; Ren, W.; Wright, Q. E.; Ai, H.-W. *J. Am. Chem. Soc.* **2013**, *135*, 14940. (d) Yu, F.; Li, P.; Wang, B.; Han, K. *J. Am. Chem. Soc.* **2013**, *135*, 7674. (e) Peng, T.; Chen, X.; Gao, L.; Zhang, T.; Wang, W.; Shen, J.; Yang, D. *Chem. Sci.* **2016**, *7*, 5407. (f) Sun, X.; Lacina, K.; Ramsamy, E. C.; Flower, S. E.; Fossey, J. S.; Qian, X.; Anslyn, E. V.; Bull, S. D.; James, T. D. *Chem. Sci.* **2015**, *6*, 2963.
- (6) (a) Gaupels, F.; Spiazzi-Vandelle, E.; Yang, D.; Delledonne, M. *Nitric Oxide* **2011**, *25*, 222. (b) Serrano, I.; Romero-Puertas, M. C.; Rodríguez-Serrano, M.; Sandalio, L. M.; Olmedilla, A. *J. Exp. Bot.* **2012**, *63*, 1479.
- (7) (a) Fabian, W. M. F.; Schuppler, S.; Wolfbeis, O. S. *J. Chem. Soc., Perkin Trans. 2* **1996**, 853. (b) Whitaker, J. E.; Haugland, R. P.; Prendergast, F. G. *Anal. Biochem.* **1991**, *194*, 330.
- (8) Chan, J.; Dodani, S. C.; Chang, C. *J. Nat. Chem.* **2012**, *4*, 973.
- (9) (a) Song, C.; Ye, Z.; Wang, G.; Yuan, J.; Guan, Y. *Chem. - Eur. J.* **2010**, *16*, 6464. (b) Zhou, X.; Kwon, Y.; Kim, G.; Ryu, J. H.; Yoon, J. *Biosens. Bioelectron.* **2015**, *64*, 285.
- (10) Pu, K.; Shuhendler, A. J.; Rao, J. *Angew. Chem., Int. Ed.* **2013**, *52*, 10325.
- (11) (a) Zhang, Q.; Zhu, Z.; Zheng, Y.; Cheng, J.; Zhang, N.; Long, Y. T.; Zheng, J.; Qian, X.; Yang, Y. *J. Am. Chem. Soc.* **2012**, *134*, 18479. (b) Zhou, J.; Li, Y.; Shen, J.; Li, Q.; Wang, R.; Xu, Y.; Qian, X. *RSC Adv.* **2014**, *4*, 51589.
- (12) (a) Dempsey, G. T.; Bates, M.; Kowtoniuk, W. E.; Liu, D. R.; Tsien, R. Y.; Zhuang, X. *J. Am. Chem. Soc.* **2009**, *131*, 18192. (b) Chen,

P.; Li, J.; Qian, Z.; Zheng, D.; Okasaki, T.; Hayami, M. *Dyes Pigm.* **1998**, *37*, 213. (c) Nani, R. R.; Kelley, J. A.; Ivanic, J.; Schnermann, M. J. *Chem. Sci.* **2015**, *6*, 6556.

(13) (a) Conley, N. R.; Biteen, J. S.; Moerner, W. E. *J. Phys. Chem. B* **2008**, *112*, 11878. (b) Fu, N.; Xiong, Y.; Squier, T. C. *J. Am. Chem. Soc.* **2012**, *134*, 18530.

(14) (a) Yuan, L.; Lin, W.; Zheng, K.; Zhu, S. *Acc. Chem. Res.* **2013**, *46*, 1462. (b) Fan, J.; Hu, M.; Zhan, P.; Peng, X. *Chem. Soc. Rev.* **2013**, *42*, 29. (c) Yu, H.; Fu, M.; Xiao, Y. *Phys. Chem. Chem. Phys.* **2010**, *12*, 7386.

(15) Johnson, L. V.; Walsh, M. L.; Bockus, B. J.; Chen, L. *J. Cell Biol.* **1981**, *88*, 526.

(16) Martin-Romero, F. J.; Gutiérrez-Martin, Y.; Henao, F.; Gutiérrez-Merino, C. *J. Fluoresc.* **2004**, *14*, 17.

(17) (a) Salonen, T.; Sareila, O.; Jalonen, U.; Kankaanranta, H.; Tuominen, R.; Moilanen, E. Br. *J. Pharmacol.* **2006**, *147*, 790. (b) Iovine, N. M.; Pursnani, S.; Voldman, A.; Wasserman, G.; Blaser, M. J.; Weinrauch, Y. *Infect. Immun.* **2008**, *76*, 986.

(18) (a) Radi, R.; Cassina, A.; Hodara, R.; Quijano, C.; Castro, L. *Free Radical Biol. Med.* **2002**, *33*, 1451. (b) Novo, E.; Parola, M. *Fibrog. Tissue Repair* **2008**, *1*, 5.